Adhesion clusters under shared linear loading: a stochastic analysis

T. Erdmann and U. S. Schwarz

Max Planck Institute of Colloids and Interfaces, 14424 Potsdam, Germany

We study the cooperative rupture of multiple adhesion bonds under shared linear loading. Simulations of the appropriate Master equation are compared with numerical integration of a rate equation for the mean number of bonds and its scaling analysis. In general, force-accelerated rupture is rather abrupt. For small clusters and slow loading, large fluctuations occur regarding the timepoint of final rupture, but not the typical shape of the rupture trajectory. For vanishing rebinding, our numerical results confirm three scaling regimes predicted before for cluster lifetime as a function of loading rate. For finite rebinding, the intermediate loading regime becomes irrelevant, and a sequence of two new scaling laws can be identified in the slow loading regime.

I. INTRODUCTION

Cell adhesion is based on a large variety of different adhesion molecules, each of which is optimised for its specific biological function [1]. Most adhesion molecules have evolved to operate under force. For example, in cell-matrix adhesion, receptors from the integrin family usually function under conditions of cellular contractility [2], while in leukocyte adhesion to blood vessel walls, receptors from the selectin family operate under shear flow [3]. During recent years, single molecule force spectroscopy has revealed formerly hidden properties of many different adhesion molecules, which in the future might be linked explicitly to their biological function [4]. Rupture of molecular bonds under force is a stochastic process which can be modeled with Kramers theory as thermally activated escape over a sequence of transition state barriers [5, 6, 7]. The most convenient loading protocol is a linear ramp of force, both experimentally and theoretically. For single molecules, the most frequent rupture force as a function of the logarithm of loading rate has been predicted to be a sequence of linear parts, each of which corresponding to one transition state barrier along the rupture path [5]. This prediction has been confirmed experimentally for many different adhesion systems [4, 8], including $\alpha_5\beta_1$-integrin [9] and L-selectin mediated bonds [10].

Although single molecule force spectroscopy has strongly changed our understanding of specific adhesion, cell adhesion is usually not based on single molecules, but on clusters of varying size. Therefore, future understanding of cell adhesion also has to include the cooperative behaviour of adhesion molecules under force. In single molecule experiments, ruptured bonds usually cannot rebind due to elastic recoil of the transducer. In contrast, ruptured bonds in adhesion clusters can rebind as long as other bonds are still closed, thus holding ligands and receptors in close proximity. For adhesion clusters under constant loading, it is well known that despite rebinding, stability is lost beyond a critical force [1]. For adhesion clusters under linear loading, force grows without bounds and the cluster will always rupture. Recently, the most frequent rupture force has been measured as a function of loading rate for clusters of $\alpha_\nu\beta_3$-integrins and RGD-lipopeptides loaded through a soft transducer in a homogeneous way [11]. Theoretically, it has been shown before that different scaling regimes exist for cluster lifetime as a function of cluster size, loading rate and rebinding rate [12]. For the case of a stiff transducer, force on single bonds is independent of the number of closed bonds and a mean field approximation can be applied to make further theoretical progress [13]. However, for the case of a soft transducer, force is shared between closed bonds, leading to real cooperativity: if one of the closed bonds ruptures, force is redistributed over the remaining closed ones. Here we present for the first time a full treatment of this case. We start with a one-step Master equation with Kramers-like rates, which is solved by Monte Carlo methods. These results are then compared to numerical integration of a rate equation for the mean number of bonds. We show that considerable differences exist between the stochastic and deterministic treatments for small clusters or slow loading. For the case of vanishing rebinding, our results confirm the three scaling regimes for cluster lifetime as a function of loading rate, which have been predicted before on the basis of a scaling analysis of the rate equation for the mean number of bonds [12]. For the case of finite rebinding, the intermediate scaling regime becomes irrelevant. For slow loading, we identify a sequence of two new scaling laws, which result from stochastic decay towards an absorbing boundary and finite rupture strength at constant loading, respectively.

II. MODEL

We consider a cluster with N_t parallel bonds. At any time t, i bonds are closed and $N_t - i$ bonds are open ($0 \leq i \leq N_t$). The i closed bonds are assumed to share force F equally, that is each closed bond is subject to the force F/i. In the following, we will consider linear loading, that is $F = rt$ where r is loading rate. Single closed bonds are assumed to rupture with the dissociation rate $k = k_0 e^{F/iF_b}$, which corresponds to the case of one sharp transition
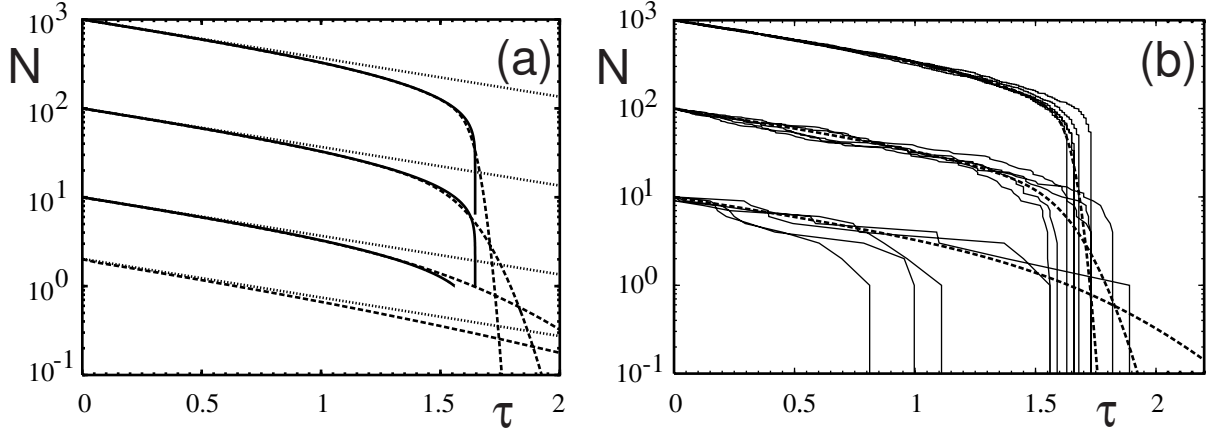
FIG. 1: (a) Mean number of closed bonds N as a function of time τ for the case of vanishing rebinding, $\gamma = 0$, for $\mu/N_0 = 0.1$ and $N_t = N_0 = 2, 10, 10^2$ and 10^3. Dotted lines: Initial exponential decay. Dashed lines: first moment of the Monte Carlo simulations. Solid lines: numerical integration of deterministic rate equation (not for $N_t = 2$). (b) Individual trajectories from Monte Carlo simulations in comparison with the mean (not for $N_t = 2$).

state barrier along the rupture path [1, 5]. Here, F_b is the internal force scale of the bond set by the barrier. Single open bonds are assumed to rebind with the force independent association rate k_{on}. We now introduce dimensionless variables: dimensionless time $\tau = k_0 t$, dimensionless loading rate $\mu = r/k_0 F_b$ and dimensionless rebinding rate $\gamma = k_{on}/k_0$. The stochastic dynamics of our model is described by a one-step Master equation

$$\frac{dp_i}{d\tau} = r_{i+1}p_{i+1} + g_{i-1}p_{i-1} - [r_i + g_i]p_i \tag{1}$$

where $p_i(\tau)$ is the probability that i closed bonds are present at time τ. The reverse and forward rates between the different states i follow from the single molecule rates as

$$r_i = i e^{\mu\tau/i} \quad \text{and} \quad g_i = \gamma(N_t - i) . \tag{2}$$

For constant force, this Master equation has been studied before [14, 15]. Since adhesion clusters (like single molecules) usually cannot rebind from the completely dissociated state due to elastic recoil of the transducer, we implement an absorbing boundary at $i = 0$ by setting $g_0 = 0$. Since force increases in time without bounds, the cluster will always dissociate in the long run, that is $p_i(\tau) \to \delta_{i0}$ for $\tau \to \infty$, both for absorbing and reflecting boundaries. Cluster lifetime T is the mean time to reach the absorbing state $i = 0$. By defining cluster dissociation rate $D = dp_0/d\tau = r_1 p_1$, cluster lifetime follows as $T = \int_0^\infty d\tau\ \tau D$. Since the reverse rates r_i are non-linear in i and time-dependent, an analytical solution for the p_i as a function of the three model parameters N_t, μ and γ seems to be impossible. Therefore we solve the Master equation numerically using the Gillespie algorithm for efficient Monte Carlo simulations, typically averaging over 10^5 simulation trajectories for each set of parameters [16].

A quantity of large interest is the mean number of closed bonds, $N = \langle i \rangle = \sum_{i=1}^{N_t} i p_i$. In a continuum approach, one expects that this quantity satisfies the ordinary differential equation

$$\frac{dN}{d\tau} = -N e^{\mu\tau/N} + \gamma(N_t - N) . \tag{3}$$

Cluster lifetime T can be defined by $N(T) = 1$. Several different scaling regimes for T as a function of N_t, μ and γ have been predicted on the basis of Eq. (3) [12]. Below these scaling predictions will be compared to both numerical integration of the deterministic equation and to our stochastic results.

III. DECAY WITHOUT REBINDING

We first consider the case of vanishing rebinding, $\gamma = 0$. In this case the total number of bonds N_t does not appear in the model equations and the initial condition $N(0) = N_0$ is the only relevant parameter concerning the number of bonds. The scaling analysis of Eq. (3) suggests that decay can be divided into two parts [12]. Initial decay is not yet
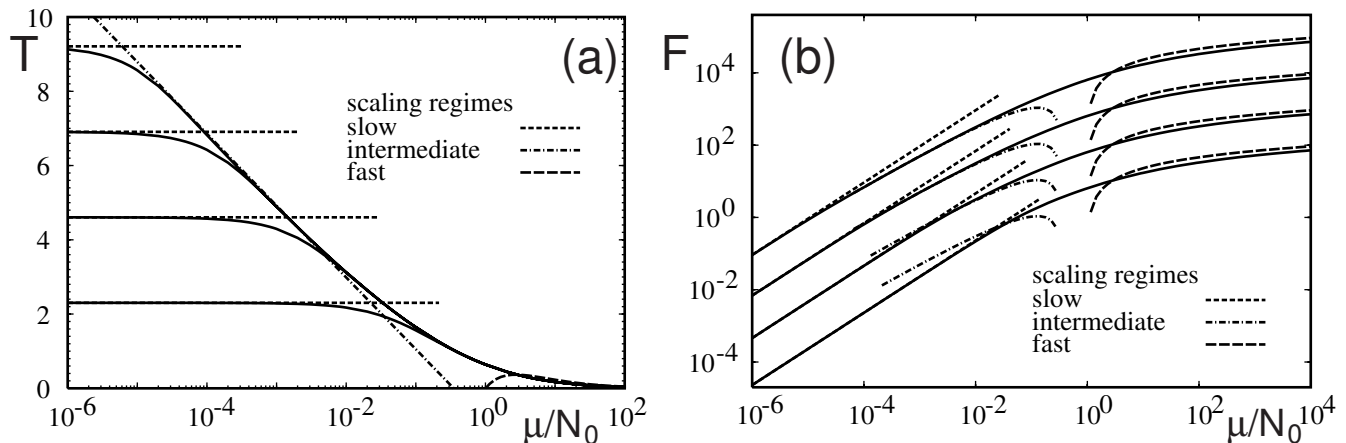
FIG. 2: Solid lines: deterministic results for (a) cluster lifetime T and (b) rupture force $F = \mu T$ for the case of vanishing rebinding, $\gamma = 0$, as a function of μ/N_0 for $N_t = N_0 = 10, 10^2, 10^3$ and 10^4. Dashed lines: curves for all three scaling regimes.

affected by loading and thus is exponential with $N(\tau) = N_0 e^{-\tau}$. The second part of the decay is super-exponential and can be shown to be much shorter than the first one. Therefore the crossover time, which is defined by an implicit function, determines cluster lifetime T. In the regime of slow loading, $\mu < 1$, exponential decay persists until $N(\tau) = 1$ and $T = \ln N_0$. In the regime of intermediate loading, $1 < \mu < N_0$, the crossover occurs before $N(\tau) = 1$ is reached, and lifetime is reduced to $T \sim \ln(N_0/\mu)$. In the regime of fast loading, $\mu > N_0$, lifetime scales even stronger with loading rate, $T \sim (N_0/\mu) \ln(\mu/N_0)$.

In Fig. 1a we plot $N(\tau)$ as obtained from simulations of the Master equation (dashed lines) and from numerical integration of the deterministic equation (solid lines) for $N_0 = 2, 10, 10^2$ and 10^3. The dotted lines are the exponential decays $N(\tau) = N_0 e^{-\tau}$ for vanishing loading. In the presence of loading, the later part of the decay process clearly is super-exponential. The first moment of the stochastic process decays less abrupt than the deterministic result, although for increasing cluster size, the difference between stochastic and deterministic results becomes smaller. In Fig. 1b, we show representative trajectories from Monte Carlo simulations. They demonstrate that the final stage of the rupture process is rather abrupt. In fact abrupt decay is typical for shared loading and is found also for shared *constant* loading: a decreasing number of closed bonds increases force on the remaining bonds, thus further increasing their dissociation rates [15]. As Fig. 1b shows, fluctuations tend to change the timepoint of rupture, rather than the typical shape of the decay curve. For increasing cluster size, fluctuations become smaller and rupture events are concentrated around the rupture of the deterministic cluster. An analysis of the variance of the number of closed bonds i shows that for slow loading, it is close to the exact result for vanishing loading, $\langle i^2 \rangle - \langle i \rangle^2 = N_0 e^{-\tau}(1 - e^{-\tau})$ [17]. It vanishes for $\tau = 0$ due to the initial condition, then quickly rises to a maximum and finally decays exponentially. As loading rate μ increases, a large additional peak appears shortly before final rupture (not shown).

Simulations allow to measure cluster dissociation rate $D(\tau)$ and cluster lifetime T for all parameter values. For $\mu < 1$, the simulation results are close to the known analytical results for $\mu = 0$, $D(\tau) = N_0 e^{-\tau}(1 - e^{-\tau})^{N_0-1}$ [17] and $T = \sum_{i=1}^{N_0} 1/i \approx \ln N_0 + (1/2N_0) + 0.577$ [18, 19]. For large N_0, the deterministic scaling $T = \ln N_0$ results. For $\mu > 1$, the functions $D(\tau)$ become narrowly peaked around the mean value T. As suggested by the scaling analysis, we find that now T depends only on the value of μ/N_0. In Fig. 2a, we plot deterministic results for T as a function of μ/N_0 and for different values of N_0. The stochastic results are very similar, except for the differences in the initial plateau values. Initially, the different curves plateau at the values $\ln N_0$ for $\mu < 1$. For $1 < \mu < N_0$ and sufficiently large N_0, they collapse onto a universal curve, which can be approximated by $0.84 \ln(0.35 N_0/\mu)$. For $\mu > N_0$, they collapse onto another universal curve, $(N_0/\mu) \ln(\mu/N_0)$. In Fig. 2b, we plot the logarithm of the deterministic rupture force, $F = \mu T$, as a function of μ/N_0. For large N_0, one clearly sees the sequence of the three different scaling regimes. For decreasing N_0, the intermediate scaling curve becomes an increasingly bad fit.

IV. EFFECT OF REBINDING

In the stochastic framework, cluster lifetime can be identified with the finite mean first passage time of reaching the absorbing boundary at $i = 0$. For $\mu = 0$ and $N_0 = N_t$, an exact result can be obtained with the help of Laplace
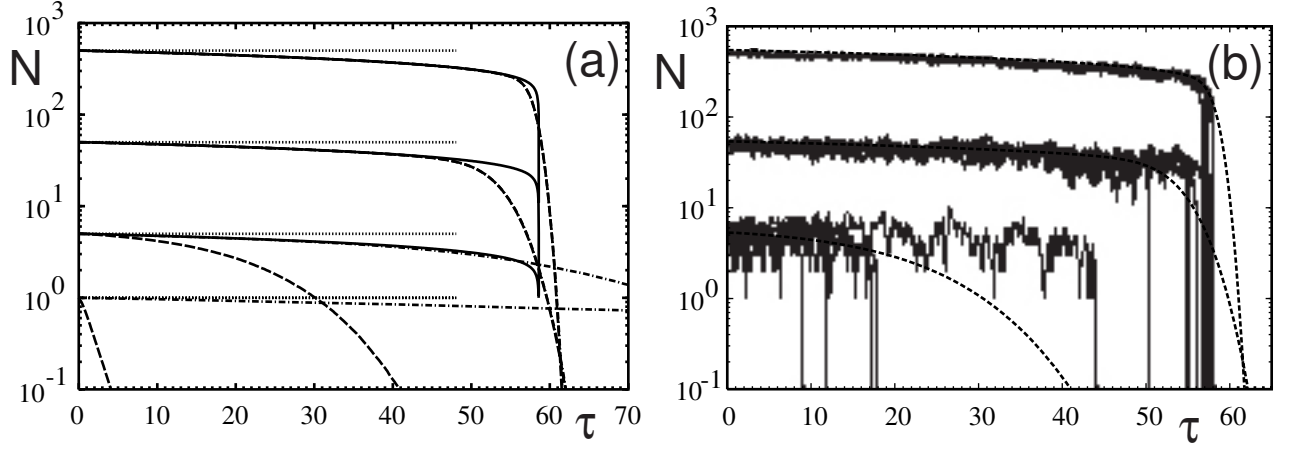
FIG. 3: (a) Mean number of closed bonds N as a function of time τ for rebinding rate $\gamma = 1$ and loading rate $\mu/N_0 = 0.01$. Cluster sizes $N_t = 2, 10, 10^2$ and 10^3, initial condition $N_0 = N_{eq} = \gamma N_t/(1 + \gamma)$. Dotted lines: Initial number of closed bonds. Dashed lines: first moment of the Monte Carlo simulations. Solid lines: numerical integration of deterministic equation (not for $N_t = 2$). Dashed-dotted lines: effect of reflecting boundary for $N_t = 2$ and 10. (b) Individual trajectories from Monte Carlo simulations in comparison with the mean (not for $N_t = 2$).

transforms [15]:

$$T_{stoch} = \frac{1}{1 + \gamma}\left(H_{N_t} + \sum_{i=1}^{N_t}\binom{N_t}{i}\frac{\gamma^i}{i} \right) , \tag{4}$$

where $H_{N_t} = \sum_{i=1}^{N_t}(1/i)$ is the N_tth harmonic number. In the deterministic framework of Eq. (3) and $\mu = 0$, an adhesion cluster with a total of N_t molecular bonds will equilibrate from any initial number of closed bonds N_0 to a stable steady state with $N_{eq} = \gamma N_t/(1 + \gamma)$ closed bonds. For convenience, in the following we will use $N_0 = N_{eq}$. Then similar results follow for T_{stoch} as given in Eq. (4). A stability analysis of the deterministic equation Eq. (3) for loading with a *constant* force $f = F/F_b$ shows that the steady state cluster size decreases until stability is lost beyond a critical force $f_c = N_t \text{plog}(\gamma/e)$ [1, 15]. Here the product logarithm plog(a) is defined as the solution x of $xe^x = a$. For $\gamma < 1$, the critical force can be approximated as $f_c \approx N_t\gamma/e$: it vanishes with γ since without rebinding the cluster decays by itself. For $\gamma > 1$, it can be approximated as $f_c \approx 0.5N_t \ln\gamma$, that is the critical force now is only a weak function of rebinding. For slow loading, $\mu < 1$, the adhesion cluster will follow the quasi-steady state until the critical force f_c is reached at the time $\tau_c = f_c/\mu$. The remaining time to rupture is smaller and thus the lifetime of the adhesion cluster is close to

$$T_{det} = \frac{N_t}{\mu}\text{plog}\frac{\gamma}{e} . \tag{5}$$

It diverges with the inverse of loading rate in the limit of vanishing μ, as it is required by the existence of a stable steady state and a finite rupture force $F = \mu T = f_c$. For intermediate loading, $1 < \mu < N_0$, a power-law behaviour $T \sim (N_0/\mu)^{1/2}$ has been erroneously predicted in ref. [12], as reported in ref. [13]. For fast loading, $\mu > N_0$, rebinding can be neglected and $T \sim (N_0/\mu)\ln(\mu/N_0)$ as in the previous section.

In Fig. 3a $N(\tau)$ is plotted for $\gamma = 1$ as obtained from Monte Carlo simulations (dashed lines) and from numerical integration of the deterministic equation (solid lines). The different initial conditions N_0 for $N_t = 2, 10, 10^2$ and 10^3 are represented by the dotted lines. In Fig. 3b individual trajectories from the simulations are compared to the stochastic averages from Fig. 3a. For the small clusters, $N_t = 2$ and 10, loading rate is so small that $f_c/\mu > T_{stoch}$. Then $T \approx T_{stoch}$ and the clusters decay by themselves due to stochastic fluctuations to the absorbing boundary (*ultra-slow regime*). The dash-dotted lines in Fig. 3a show the effect of a reflecting boundary, which is rather dramatic for these small cluster sizes. For the large clusters, $N_t = 10^2$ and 10^3, fluctuations are less probable until the force is close to f_c. Therefore the individual clusters fluctuate around the quasi-steady state and dissociate only close to the deterministic cluster lifetime T_{det}. Due to the large force on a single bond at f_c, the boundary has little influence here. A detailed analysis of the variance of i confirms this description (not shown): for the smallest cluster, when fluctuations dominate during the whole time evolution, the variance shows a broad peak. For the larger clusters, it develops a narrow peak around the mean rupture time.
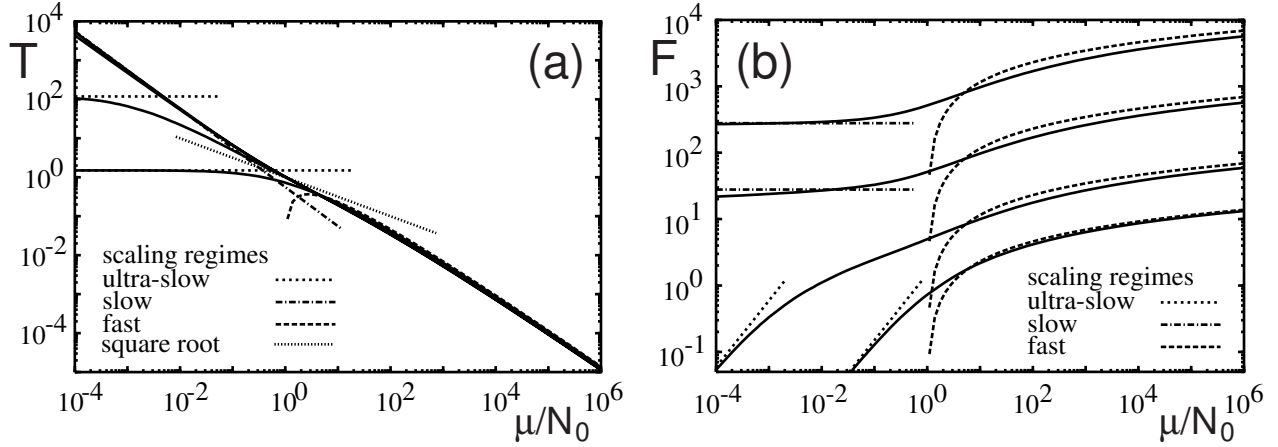
FIG. 4: (a) Mean cluster lifetime T and (b) mean rupture force $F = \mu T$ for the case $\gamma = 1$ as a function of μ/N_0 for $N_t = 2, 10, 10^2$ and 10^3. In (a), the curves for the two larger clusters are nearly identical.

In Fig. 4, we show mean cluster lifetime T and mean rupture force $F = \mu T$ for $\gamma = 1$ as a function of μ/N_0 for the cases $N_t = 2, 10, 10^2$ and 10^3. For the small clusters, T starts at the value of T_{stoch} and ends in the scaling regime for fast loading, where the curves are practically identical for all different parameter values at a given value for μ/N_0. The curves for the large clusters are nearly identical. They start at the values of T_{det} for small loading rates and end in the same fast loading regime. An intermediate loading regime seems to exist only as a transient between the regimes of slow and fast loading. In particular, it does not fit well to an inverse square root dependence, as shown in Fig. 4a.

V. CONCLUSIONS

In this paper, we have presented for the first time a full analysis of the cooperative decay of a cluster of adhesion bonds under linearly rising force. Significant differences between stochastic and deterministic treatments are found for small clusters or slow loading, when stochastic fluctuations are relevant. However, they do not affect so much the typical shape of the rupture trajectory, but rather the timepoint at which rupture occurs. For the case of vanishing rebinding, $\gamma = 0$, our full treatment nicely confirms the scaling analysis of the deterministic equation for cluster lifetime T as a function of μ and N_0 [12]. However, in contrast to the scaling analysis, the full treatment presented here allows for detailed comparision with experiments, e.g. in regard to typical unbinding trajectories or binding strength over a range of loading rates spanning different scaling regimes. For the case with finite rebinding, $\gamma > 0$, we identify a sequence of two new scaling laws within the regime of slow loading, $\mu < 1$. For ultra-slow loading, T is independent of μ and is determined by stochastic fluctuations towards the absorbing boundary. For larger μ (but still with $\mu < 1$), T starts to scale inversely with μ, due to the finite rupture strength at constant loading. In contrast to the case of vanishing rebinding, a scaling regime of intermediate loading, $1 < \mu < N_0$, could not be identified.

Our results can be applied for example to rolling adhesion of leukocytes, when multiple L-selectin bonds are dynamically loaded in shear flow [20]. Dynamic force spectroscopy has only recently been applied to clusters of adhesion bonds [11]. RGD-lipopeptides on a vesicle have been presented to $\alpha_\nu\beta_3$-integrins on a cell. The effect of thermal membrane fluctuations can be disregarded on both sides, because the vesicle is under large tension and the integrins are rigidly connected to the cytoskeleton. Appreciable loading occurs only over a ring region along the rim of the contact disc, for which no inhomogeneities have been observed. If one neglects the subsequent peeling of the inner region, which presumably is much faster, our model can be applied. The parameter values can be estimated to be $N_t \approx 100$, $F_b \approx 40$ pN, $k_0 \approx 0.01$ Hz and $\gamma \approx 1$. Loading rates have been varied from $r = 20 - 4 \times 10^3$ pN/s, that is $\mu/N_t = 0.5 - 100$. Therefore this experiment should correspond to the intermediate and fast loading regimes. We expect that future improvements in experimentation will make it possible to probe also the slow loading regime, where rebinding and stochastic effects become relevant. In order to achieve a more complete understanding of the role of force in cell adhesion, future modeling should also address the detailed nature of the force transducer, non-homogeneous loading and more realistic scenarios for the rebinding process.

Acknowledgments

[1] G. I. Bell. Models for the specific adhesion of cells to cells. *Science*, 200:618–627, 1978.

[2] B. Geiger and A. Bershadsky. Exploring the neighborhood: adhesion-coupled cell mechanosensors. *Cell*, 110:139–142, 2002.

[3] H. Rossiter, R. Alon, and T. S. Kupper. Selectins, T-cell rolling and inflammation. *Molec. Med. Today*, 3:214–222, 1997.

[4] E. Evans. Probing the relation between force, lifetime and chemistry in single molecular bonds. *Annu. Rev. Biophys. Biomol. Struct.*, 30:105–28, 2001.

[5] E. Evans and K. Ritchie. Dynamic strength of molecular adhesion bonds. *Biophys. J.*, 72:1541–1555, 1997.

[6] S. Izrailev, S. Stepaniants, M. Balsera, Y. Oono, and K. Schulten. Molecular dynamics study of unbinding of the avidin-biotin complex. *Biophys. J.*, 72:1568–1581, 1997.

[7] J. Shillcock and U. Seifert. Escape from a metastable well under a time-ramped force. *Phys. Rev. E*, 57:7301–7304, 1998.

[8] R. Merkel, P. Nassoy, A. Leung, K. Ritchie, and E. Evans. Energy landscapes of receptor-ligand bonds explored with dynamic force spectroscopy. *Nature*, 397:50–53, 1999.

[9] F. Li, S. D. Redick, H. P. Erickson, and V. T. Moy. Force measurements of the $\alpha_5\beta_1$ integrin-fibronectin interaction. *Biophys. J.*, 84:1252–1262, 2003.

[10] E. Evans, A. Leung, D. Hammer, and S. Simon. Chemically distinct transition states govern rapid dissociation of single L-selectin bonds under force. *Proc. Natl. Acad. Sci. USA*, 98:3784–3789, 2001.

[11] K. Prechtel, A. R. Bausch, V. Marchi-Artzner, M. Kantlehner, H. Kessler, and R. Merkel. Dynamic force spectroscopy to probe adhesion strength of living cells. *Phys. Rev. Lett.*, 89:028101, 2002.

[12] U. Seifert. Rupture of multiple parallel molecular bonds under dynamic loading. *Phys. Rev. Lett.*, 84:2750–2753, 2000.

[13] U. Seifert. Dynamic strength of adhesion molecules: role of rebinding and self-consistent rates. *Europhys. Lett.*, 58:792–798, 2002.

[14] C. Cozens-Roberts, D. A. Lauffenburger, and J. A. Quinn. Receptor-mediated cell attachment and detachment kinetics. *Biophys. J.*, 58:841–872, 1990.

[15] T. Erdmann and U. S. Schwarz. Stability of adhesion clusters under constant force. *Phys. Rev. Lett.*, 92:108102, 2004.

[16] D. T. Gillespie. Exact stochastic simulation of coupled chemical reactions. *J. Phys. Chem.*, 81:2340–2361, 1977.

[17] D. A. McQuarrie. Kinetics of small systems I. *J. Chem. Phys.*, 38:433–436, 1963.

[18] B. Goldstein and C. Wofsy. Why is it so hard to dissociate multivalent antigens from cell-surface antibodies ? *Immunology Today*, 17:77–80, 1996.

[19] D. F. J. Tees, J. T. Woodward, and D. A. Hammer. Reliability theory for receptor-ligand bond dissociation. *J. Chem. Phys.*, 114:7483–7496, 2001.

[20] O. Dwir, A. Solomon, S. Mangan, G. S. Kansas, U. S. Schwarz, and R. Alon. Avidity enhancement of L-selectin bonds by flow: shear-promoted rotation of leukocytes turn labile bonds into functional tethers. *J. Cell Biol.*, 163:649–659, 2003.